Measurement of the Differential Cross Section d /d(cos t) for Top-Quark Pair Production in pp⁻ Collisions at s√=1.96 TeV

CDF Collaboration ; et al ; Canelli, F ; Kilminster, B

Abstract: We report a measurement of the differential cross section d /d(cos t) for top-quark pair production as a function of the top-quark production angle in proton-antiproton collisions at s√=1.96 TeV. This measurement is performed using data collected with the CDF II detector at the Tevatron, corresponding to an integrated luminosity of 9.4 fb−1. We employ the Legendre polynomials to characterize the shape of the differential cross section at the parton level. The observed Legendre coefficients are in good agreement with the prediction of the next-to-leading-order standard-model calculation, with the exception of an excess linear-term coefficient a1=0.40±0.12, compared to the standard-model prediction of a1=0.15+0.07−0.03.

DOI: https://doi.org/10.1103/PhysRevLett.111.182002

Measurement of the Differential Cross Section $d\sigma/d(\cos\theta_t)$ for Top-Quark Pair Production in $p\bar{p}$ Collisions at $\sqrt{s} = 1.96\,\mathrm{TeV}$

T. Aaltonen,[21] S. Amerio[jj],[39] D. Amidei,[31] A. Anastassov[v],[15] A. Annovi,[17] J. Antos,[12] G. Apollinari,[15] J.A. Appel,[15] T. Arisawa,[52] A. Artikov,[13] J. Asaadi,[47] W. Ashmanskas,[15] B. Auerbach,[2] A. Aurisano,[47] F. Azfar,[38] W. Badgett,[15] T. Bae,[25] A. Barbaro-Galtieri,[26] V.E. Barnes,[43] B.A. Barnett,[23] P. Barria[ll],[41] P. Bartos,[12] M. Bauce[jj],[39] F. Bedeschi,[41] S. Behari,[15] G. Bellettini[kk],[41] J. Bellinger,[54] D. Benjamin,[14] A. Beretvas,[15] A. Bhatti,[45] K.R. Bland,[5] B. Blumenfeld,[23] A. Bocci,[14] A. Bodek,[44] D. Bortoletto,[43] J. Boudreau,[42] A. Boveia,[11] L. Brigliadori[ii],[6] C. Bromberg,[32] E. Brucken,[21] J. Budagov,[13] H.S. Budd,[44] K. Burkett,[15] G. Busetto[jj],[39] P. Bussey,[19] P. Butti[kk],[41] A. Buzatu,[19] A. Calamba,[10] S. Camarda,[4] M. Campanelli,[28] F. Canelli[cc],[11] B. Carls,[22] D. Carlsmith,[54] R. Carosi,[41] S. Carrillo[l],[16] B. Casal[j],[9] M. Casarsa,[48] A. Castro[ii],[6] P. Catastini,[20] D. Cauz[qqrr],[48] V. Cavaliere,[22] M. Cavalli-Sforza,[4] A. Cerri[e],[26] L. Cerrito[q],[28] Y.C. Chen,[1] M. Chertok,[7] G. Chiarelli,[41] G. Chlachidze,[15] K. Cho,[25] D. Chokheli,[13] A. Clark,[18] C. Clarke,[53] M.E. Convery,[15] J. Conway,[7] M. Corbo[y],[15] M. Cordelli,[17] C.A. Cox,[7] D.J. Cox,[7] M. Cremonesi,[41] D. Cruz,[47] J. Cuevas[x],[9] R. Culbertson,[15] N. d'Ascenzo[u],[15] M. Datta[ff],[15] P. de Barbaro,[44] L. Demortier,[45] M. Deninno,[6] M. D'Errico[jj],[39] F. Devoto,[21] A. Di Canto[kk],[41] B. Di Ruzza[p],[15] J.R. Dittmann,[5] S. Donati[kk],[41] M. D'Onofrio,[27] M. Dorigo[ss],[48] A. Driutti[qqrr],[48] K. Ebina,[52] R. Edgar,[31] A. Elagin,[47] R. Erbacher,[7] S. Errede,[22] B. Esham,[22] S. Farrington,[38] J.P. Fernández Ramos,[29] R. Field,[16] G. Flanagan[s],[15] R. Forrest,[7] M. Franklin,[20] J.C. Freeman,[15] H. Frisch,[11] Y. Funakoshi,[52] C. Galloni[kk],[41] A.F. Garfinkel,[43] P. Garosi[ll],[41] H. Gerberich,[22] E. Gerchtein,[15] S. Giagu,[46] V. Giakoumopoulou,[3] K. Gibson,[42] C.M. Ginsburg,[15] N. Giokaris,[3] P. Giromini,[17] G. Giurgiu,[23] V. Glagolev,[13] D. Glenzinski,[15] M. Gold,[34] D. Goldin,[47] A. Golossanov,[15] G. Gomez,[9] G. Gomez-Ceballos,[30] M. Goncharov,[30] O. González López,[29] I. Gorelov,[34] A.T. Goshaw,[14] K. Goulianos,[45] E. Gramellini,[6] S. Grinstein,[4] C. Grosso-Pilcher,[11] R.C. Group,[51,15] J. Guimaraes da Costa,[20] S.R. Hahn,[15] J.Y. Han,[44] F. Happacher,[17] K. Hara,[49] M. Hare,[50] R.F. Harr,[53] T. Harrington-Taber[m],[15] K. Hatakeyama,[5] C. Hays,[38] J. Heinrich,[40] M. Herndon,[54] A. Hocker,[15] Z. Hong,[47] W. Hopkins[f],[15] S. Hou,[1] R.E. Hughes,[35] U. Husemann,[55] M. Hussein[aa],[32] J. Huston,[32] G. Introzzi[nnoo],[41] M. Iori[pp],[46] A. Ivanov[o],[7] E. James,[15] D. Jang,[10] B. Jayatilaka,[15] E.J. Jeon,[25] S. Jindariani,[15] M. Jones,[43] K.K. Joo,[25] S.Y. Jun,[10] T.R. Junk,[15] M. Kambeitz,[24] T. Kamon,[25,47] P.E. Karchin,[53] A. Kasmi,[5] Y. Kato[n],[37] W. Ketchum[gg],[11] J. Keung,[40] B. Kilminster[cc],[15] D.H. Kim,[25] H.S. Kim,[25] J.E. Kim,[25] M.J. Kim,[17] S.H. Kim,[49] S.B. Kim,[25] Y.J. Kim,[25] Y.K. Kim,[11] N. Kimura,[52] M. Kirby,[15] K. Knoepfel,[15] K. Kondo,[52,*] D.J. Kong,[25] J. Konigsberg,[16] A.V. Kotwal,[14] M. Kreps,[24] J. Kroll,[40] M. Kruse,[14] T. Kuhr,[24] M. Kurata,[49] A.T. Laasanen,[43] S. Lammel,[15] M. Lancaster,[28] K. Lannon[w],[35] G. Latino[ll],[41] H.S. Lee,[25] J.S. Lee,[25] S. Leo,[41] S. Leone,[41] J.D. Lewis,[15] A. Limosani[r],[14] E. Lipeles,[40] A. Lister[a],[18] H. Liu,[51] Q. Liu,[43] T. Liu,[15] S. Lockwitz,[55] A. Loginov,[55] D. Lucchesi[jj],[39] A. Lucà,[17] J. Lueck,[24] P. Lujan,[26] P. Lukens,[15] G. Lungu,[45] J. Lys,[26] R. Lysak[d],[12] R. Madrak,[15] P. Maestro[ll],[41] S. Malik,[45] G. Manca[b],[27] A. Manousakis-Katsikakis,[3] L. Marchese[hh],[6] F. Margaroli,[46] P. Marino[mm],[41] M. Martínez,[4] K. Matera,[22] M.E. Mattson,[53] A. Mazzacane,[15] P. Mazzanti,[6] R. McNulty[i],[27] A. Mehta,[27] P. Mehtala,[21] C. Mesropian,[45] T. Miao,[15] D. Mietlicki,[31] A. Mitra,[1] H. Miyake,[49] S. Moed,[15] N. Moggi,[6] C.S. Moon[y],[15] R. Moore[ddee],[15] M.J. Morello[mm],[41] A. Mukherjee,[15] Th. Muller,[24] P. Murat,[15] M. Mussini[ii],[6] J. Nachtman[m],[15] Y. Nagai,[49] J. Naganoma,[52] I. Nakano,[36] A. Napier,[50] J. Nett,[47] C. Neu,[51] T. Nigmanov,[42] L. Nodulman,[2] S.Y. Noh,[25] O. Norniella,[22] L. Oakes,[38] S.H. Oh,[14] Y.D. Oh,[25] I. Oksuzian,[51] T. Okusawa,[37] R. Orava,[21] L. Ortolan,[4] C. Pagliarone,[48] E. Palencia[e],[9] P. Palni,[34] V. Papadimitriou,[15] W. Parker,[54] G. Pauletta[qqrr],[48] M. Paulini,[10] C. Paus,[30] T.J. Phillips,[14] G. Piacentino,[41] E. Pianori,[40] J. Pilot,[7] K. Pitts,[22] C. Plager,[8] L. Pondrom,[54] S. Poprocki[f],[15] K. Potamianos,[26] A. Pranko,[26] F. Prokoshin[z],[13] F. Ptohos[g],[17] G. Punzi[kk],[41] N. Ranjan,[43] I. Redondo Fernández,[29] P. Renton,[38] M. Rescigno,[46] F. Rimondi,[6,*] L. Ristori,[41,15] A. Robson,[19] T. Rodriguez,[40] S. Rolli[h],[50] M. Ronzani[kk],[41] R. Roser,[15] J.L. Rosner,[11] F. Ruffini[ll],[41] A. Ruiz,[9] J. Russ,[10] V. Rusu,[15] W.K. Sakumoto,[44] Y. Sakurai,[52] L. Santi[qqrr],[48] K. Sato,[49] V. Saveliev[u],[15] A. Savoy-Navarro[y],[15] P. Schlabach,[15] E.E. Schmidt,[15] T. Schwarz,[31] L. Scodellaro,[9] F. Scuri,[41] S. Seidel,[34] Y. Seiya,[37] A. Semenov,[13] F. Sforza[kk],[41] S.Z. Shalhout,[7] T. Shears,[27] P.F. Shepard,[42] M. Shimojima[t],[49] M. Shochet,[11] I. Shreyber-Tecker,[33] A. Simonenko,[13] K. Sliwa,[50] J.R. Smith,[7] F.D. Snider,[15] H. Song,[42] V. Sorin,[4] R. St. Denis,[19] M. Stancari,[15] D. Stentz[v],[15] J. Strologas,[34] Y. Sudo,[49] A. Sukhanov,[15] I. Suslov,[13] K. Takemasa,[49] Y. Takeuchi,[49] J. Tang,[11] M. Tecchio,[31] P.K. Teng,[1] J. Thom[f],[15] E. Thomson,[40] V. Thukral,[47] D. Toback,[47] S. Tokar,[12] K. Tollefson,[32] T. Tomura,[49] D. Tonelli[e],[15] S. Torre,[17] D. Torretta,[15] P. Totaro,[39] M. Trovato[mm],[41] F. Ukegawa,[49] S. Uozumi,[25] F. Vázquez[l],[16] G. Velev,[15] C. Vellidis,[15]

C. Vernieri[mm],[41] M. Vidal,[43] R. Vilar,[9] J. Vizán[bb],[9] M. Vogel,[34] G. Volpi,[17] P. Wagner,[40] R. Wallny[j],[15] S.M. Wang,[1] D. Waters,[28] W.C. Wester III,[15] D. Whiteson[c],[40] A.B. Wicklund,[2] S. Wilbur,[7] H.H. Williams,[40] J.S. Wilson,[31] P. Wilson,[15] B.L. Winer,[35] P. Wittich[f],[15] S. Wolbers,[15] H. Wolfe,[35] T. Wright,[31] X. Wu,[18] Z. Wu,[5] K. Yamamoto,[37] D. Yamato,[37] T. Yang,[15] U.K. Yang,[25] Y.C. Yang,[25] W.-M. Yao,[26] G.P. Yeh,[15] K. Yi[m],[15] J. Yoh,[15] K. Yorita,[52] T. Yoshida[k],[37] G.B. Yu,[14] I. Yu,[25] A.M. Zanetti,[48] Y. Zeng,[14] C. Zhou,[14] and S. Zucchelli[ii6]

(CDF Collaboration)[†]

[1] *Institute of Physics, Academia Sinica, Taipei, Taiwan 11529, Republic of China*
[2] *Argonne National Laboratory, Argonne, Illinois 60439, USA*
[3] *University of Athens, 157 71 Athens, Greece*
[4] *Institut de Fisica d'Altes Energies, ICREA, Universitat Autonoma de Barcelona, E-08193, Bellaterra (Barcelona), Spain*
[5] *Baylor University, Waco, Texas 76798, USA*
[6] *Istituto Nazionale di Fisica Nucleare Bologna,* [ii] *University of Bologna, I-40127 Bologna, Italy*
[7] *University of California, Davis, Davis, California 95616, USA*
[8] *University of California, Los Angeles, Los Angeles, California 90024, USA*
[9] *Instituto de Fisica de Cantabria, CSIC-University of Cantabria, 39005 Santander, Spain*
[10] *Carnegie Mellon University, Pittsburgh, Pennsylvania 15213, USA*
[11] *Enrico Fermi Institute, University of Chicago, Chicago, Illinois 60637, USA*
[12] *Comenius University, 842 48 Bratislava, Slovakia; Institute of Experimental Physics, 040 01 Kosice, Slovakia*
[13] *Joint Institute for Nuclear Research, RU-141980 Dubna, Russia*
[14] *Duke University, Durham, North Carolina 27708, USA*
[15] *Fermi National Accelerator Laboratory, Batavia, Illinois 60510, USA*
[16] *University of Florida, Gainesville, Florida 32611, USA*
[17] *Laboratori Nazionali di Frascati, Istituto Nazionale di Fisica Nucleare, I-00044 Frascati, Italy*
[18] *University of Geneva, CH-1211 Geneva 4, Switzerland*
[19] *Glasgow University, Glasgow G12 8QQ, United Kingdom*
[20] *Harvard University, Cambridge, Massachusetts 02138, USA*
[21] *Division of High Energy Physics, Department of Physics, University of Helsinki, FIN-00014, Helsinki, Finland; Helsinki Institute of Physics, FIN-00014, Helsinki, Finland*
[22] *University of Illinois, Urbana, Illinois 61801, USA*
[23] *The Johns Hopkins University, Baltimore, Maryland 21218, USA*
[24] *Institut für Experimentelle Kernphysik, Karlsruhe Institute of Technology, D-76131 Karlsruhe, Germany*
[25] *Center for High Energy Physics: Kyungpook National University, Daegu 702-701, Korea; Seoul National University, Seoul 151-742, Korea; Sungkyunkwan University, Suwon 440-746, Korea; Korea Institute of Science and Technology Information, Daejeon 305-806, Korea; Chonnam National University, Gwangju 500-757, Korea; Chonbuk National University, Jeonju 561-756, Korea; Ewha Womans University, Seoul, 120-750, Korea*
[26] *Ernest Orlando Lawrence Berkeley National Laboratory, Berkeley, California 94720, USA*
[27] *University of Liverpool, Liverpool L69 7ZE, United Kingdom*
[28] *University College London, London WC1E 6BT, United Kingdom*
[29] *Centro de Investigaciones Energeticas Medioambientales y Tecnologicas, E-28040 Madrid, Spain*
[30] *Massachusetts Institute of Technology, Cambridge, Massachusetts 02139, USA*
[31] *University of Michigan, Ann Arbor, Michigan 48109, USA*
[32] *Michigan State University, East Lansing, Michigan 48824, USA*
[33] *Institution for Theoretical and Experimental Physics, ITEP, Moscow 117259, Russia*
[34] *University of New Mexico, Albuquerque, New Mexico 87131, USA*
[35] *The Ohio State University, Columbus, Ohio 43210, USA*
[36] *Okayama University, Okayama 700-8530, Japan*
[37] *Osaka City University, Osaka 558-8585, Japan*
[38] *University of Oxford, Oxford OX1 3RH, United Kingdom*
[39] *Istituto Nazionale di Fisica Nucleare, Sezione di Padova,* [jj] *University of Padova, I-35131 Padova, Italy*
[40] *University of Pennsylvania, Philadelphia, Pennsylvania 19104, USA*
[41] *Istituto Nazionale di Fisica Nucleare Pisa,* [kk] *University of Pisa,* [ll] *University of Siena,* [mm] *Scuola Normale Superiore, I-56127 Pisa, Italy,* [nn] *INFN Pavia, I-27100 Pavia, Italy,* [oo] *University of Pavia, I-27100 Pavia, Italy*
[42] *University of Pittsburgh, Pittsburgh, Pennsylvania 15260, USA*
[43] *Purdue University, West Lafayette, Indiana 47907, USA*
[44] *University of Rochester, Rochester, New York 14627, USA*
[45] *The Rockefeller University, New York, New York 10065, USA*

[46] *Istituto Nazionale di Fisica Nucleare, Sezione di Roma 1,*
[pp] Sapienza Università di Roma, I-00185 Roma, Italy
[47] *Mitchell Institute for Fundamental Physics and Astronomy,*
Texas A&M University, College Station, Texas 77843, USA
[48] *Istituto Nazionale di Fisica Nucleare Trieste, [qq] Gruppo Collegato di Udine,*
[rr] University of Udine, I-33100 Udine, Italy, [ss] University of Trieste, I-34127 Trieste, Italy
[49] *University of Tsukuba, Tsukuba, Ibaraki 305, Japan*
[50] *Tufts University, Medford, Massachusetts 02155, USA*
[51] *University of Virginia, Charlottesville, Virginia 22906, USA*
[52] *Waseda University, Tokyo 169, Japan*
[53] *Wayne State University, Detroit, Michigan 48201, USA*
[54] *University of Wisconsin, Madison, Wisconsin 53706, USA*
[55] *Yale University, New Haven, Connecticut 06520, USA*

(Dated: November 7, 2013)

We report a measurement of the differential cross section, $d\sigma/d(\cos\theta_t)$, for top-quark-pair production as a function of the top-quark production angle in proton-antiproton collisions at $\sqrt{s} = 1.96\,\text{TeV}$. This measurement is performed using data collected with the CDF II detector at the Tevatron, corresponding to an integrated luminosity of $9.4\,\text{fb}^{-1}$. We employ the Legendre polynomials to characterize the shape of the differential cross section at the parton level. The observed Legendre coefficients are in good agreement with the prediction of the next-to-leading-order standard-model calculation, with the exception of an excess linear-term coefficient, $a_1 = 0.40 \pm 0.12$, compared to the standard-model prediction of $a_1 = 0.15^{+0.07}_{-0.03}$.

PACS numbers: 14.65.Ha, 11.30.Er, 12.38.Qk

The Collider Detector at Fermilab (CDF) and D0 experiments have measured an anomalously large forward-backward asymmetry (A_{FB}) in top-quark-pair ($t\bar{t}$) hadroproduction. The latest measurements are $A_{\text{FB}} = (16.4 \pm 4.5)\,\%$ from CDF [1], and $A_{\text{FB}} = (19.6 \pm 6.5)\,\%$ from D0 [2]. This asymmetry is the manifestation of a charge asymmetry in $t\bar{t}$ production via the *CP*-even [3] initial state at the Fermilab Tevatron proton-antiproton ($p\bar{p}$) collider. The standard model (SM) [4] predicts a small forward-backward asymmetry, $(8.8 \pm 0.6)\,\%$, at next-to-leading order (NLO) in the strong coupling constant, α_s [5, 6]. The tension between the Tevatron measurements and the predictions has stimulated new work on the SM calculation [7–10] and on possible non-SM sources for the asymmetry [11]. The charge asymmetry is also under study at the LHC, but any effects are expected to be much smaller due to the forward-backward symmetric (proton-proton) initial state [12], and the results are so far inconclusive [13, 14].

We measure the differential cross section, $d\sigma/d(\cos\theta_t)$, where θ_t is the angle between the top-quark momentum and the incoming proton momentum as measured in the $t\bar{t}$ center-of-mass frame. The inclusive measurements of A_{FB} are equivalent to a two-bin measurement of this differential cross section, with one bin forward ($\cos\theta_t > 0$) and one bin backward ($\cos\theta_t < 0$). The full shape of the differential cross section provides additional information, and has the potential to discriminate among various calculations of the SM as well as models of non-SM physics. One of the aims of this study is to identify what aspects of the shape of $d\sigma/d(\cos\theta_t)$ explain the A_{FB}.

We characterize the shape of $d\sigma/d(\cos\theta_t)$ by employing the Legendre polynomials [15], which are fundamental to the general theory of scattering of particles in the present spin-averaged case [16]. The orthonormality of these

* Deceased
† With visitors from [a] University of British Columbia, Vancouver, BC V6T 1Z1, Canada, [b] Istituto Nazionale di Fisica Nucleare, Sezione di Cagliari, 09042 Monserrato (Cagliari), Italy, [c] University of California Irvine, Irvine, CA 92697, USA, [d] Institute of Physics, Academy of Sciences of the Czech Republic, 182 21, Czech Republic, [e] CERN, CH-1211 Geneva, Switzerland, [f] Cornell University, Ithaca, NY 14853, USA, [g] University of Cyprus, Nicosia CY-1678, Cyprus, [h] Office of Science, U.S. Department of Energy, Washington, DC 20585, USA, [i] University College Dublin, Dublin 4, Ireland, [j] ETH, 8092 Zürich, Switzerland, [k] University of Fukui, Fukui City, Fukui Prefecture, Japan 910-0017, [l] Universidad Iberoamericana, Lomas de Santa Fe, México, C.P. 01219, Distrito Federal, [m] University of Iowa, Iowa City, IA 52242, USA, [n] Kinki University, Higashi-Osaka City, Japan 577-8502, [o] Kansas State University, Manhattan, KS 66506, USA, [p] Brookhaven National Laboratory, Upton, NY 11973, USA, [q] Queen Mary, University of London, London, E1 4NS, United Kingdom, [r] University of Melbourne, Victoria 3010, Australia, [s] Muons, Inc., Batavia, IL 60510, USA, [t] Nagasaki Institute of Applied Science, Nagasaki 851-0193, Japan, [u] National Research Nuclear University, Moscow 115409, Russia, [v] Northwestern University, Evanston, IL 60208, USA, [w] University of Notre Dame, Notre Dame, IN 46556, USA, [x] Universidad de Oviedo, E-33007 Oviedo, Spain, [y] CNRS-IN2P3, Paris, F-75205 France, [z] Universidad Tecnica Federico Santa Maria, 110v Valparaiso, Chile, [aa] The University of Jordan, Amman 11942, Jordan, [bb] Universite catholique de Louvain, 1348 Louvain-La-Neuve, Belgium, [cc] University of Zürich, 8006 Zürich, Switzerland, [dd] Massachusetts General Hospital, Boston, MA 02114 USA, [ee] Harvard Medical School, Boston, MA 02114 USA, [ff] Hampton University, Hampton, VA 23668, USA, [gg] Los Alamos National Laboratory, Los Alamos, NM 87544, USA, [hh] Università degli Studi di Napoli Federico I, I-80138 Napoli, Italy

polynomials on the interval $[-1, 1]$ allows a unique decomposition of the cross section into a Legendre polynomial series. We write

$$\frac{d\sigma}{d(\cos\theta_t)} = \sum_{\ell=0}^{\infty} a_\ell P_\ell(\cos\theta_t), \quad (1)$$

where P_ℓ is the Legendre polynomial of degree ℓ, and a_ℓ is the Legendre moment of degree ℓ. Because the experimental sensitivity degrades as ℓ increases, we restrict the sum to $\ell \leq 8$. Since the moment a_0 contains only the total cross section, we scale all the moments so that $a_0 = 1$.

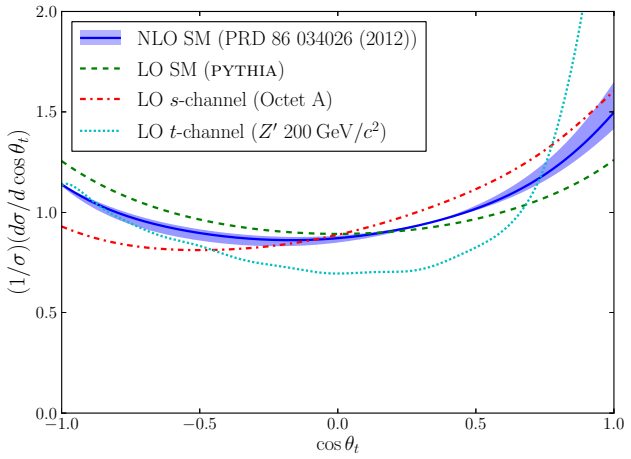

FIG. 1. The predicted differential cross sections of the LO SM [17], NLO SM [5], and benchmark models for s- and t-channel new physics [18, 19]. The band around the NLO SM prediction represents the uncertainty due to renormalization-scale choice.

At leading order (LO) in the SM, the differential cross section for $q\bar{q} \to t\bar{t}$ is

$$\frac{d\sigma^{q\bar{q}\to t\bar{t}}}{d\Omega}(\cos\theta_t, \hat{s}) = \frac{\beta\alpha_s^4}{144\pi\hat{s}}\left[2 - \beta^2(1 + \cos^2\theta_t)\right], \quad (2)$$

where β is the velocity of the top quark in units of c [20] and $\hat{s}$ is the Mandelstam variable [21]. After integrating over $\hat{s}$ to obtain $d\sigma/d(\cos\theta_t)$ and comparing to the Legendre polynomials, we expect non-zero values only for a_0 and a_2. The addition of the $gg \to t\bar{t}$ process is expected to add small contributions to all the even-degree Legendre moments. We study the LO SM via a sample of simulated events generated by PYTHIA [17]. At next-to-leading order in the SM, additional contributions to all the Legendre moments appear, including the odd moments. These non-zero odd moments introduce the lowest-order contributions to $A_{\rm FB}$. The NLO SM theoretical calculation adopted in this Letter includes the full effects of both quantum chromodynamics and the electroweak theory [5].

A wide variety of non-SM proposals has been put forward to explain the large value of $A_{\rm FB}$ observed at the Tevatron. These form two broad classes, depending on whether the new physics is dominated by s- or t-channel exchange. In order to characterize the effect of these models on the differential cross section, we study two representative models. An s-channel model, "Octet A", hypothesizes the existence of a heavy ($m_{G'} = 2\,\text{TeV}/c^2$) partner of the gluon with axial-vector couplings to quarks [18]. This produces an enhanced linear-term coefficient, a_1, in $d\sigma/d(\cos\theta_t)$ [20]. A t-channel model, "Z' 200", contains a new, heavy ($m_{Z'} = 200\,\text{GeV}/c^2$) vector boson with a flavor changing u–Z'–t coupling [19]. The resulting additional term in the cross section has a leading dependence $\hat{s}/\hat{t} = 1/(1 - \cos\theta_t)$, where $\hat{t}$ is the Mandelstam variable [21]. This behavior produces large Legendre moments at all degrees. These leading behaviors are generic predictions of s- and t-channel models [20]. Both models are studied via samples of simulated events generated at LO by MADGRAPH [22]. The LO and NLO SM calculations, as well as these two benchmark non-SM models, are shown in Figs. 1 and 2.

We study the full sample of top-quark-pair candidate events in the decay channel with a single lepton in the final state collected by the CDF experiment during Run II of the Fermilab Tevatron. The CDF II detector is a general purpose particle detector employing a large charged-particle tracking volume inside a solenoidal magnetic field coaxial with the beam direction, surrounded by calorimeters and muon detectors [23, 24]. The collected data correspond to an integrated luminosity of $9.4\,\text{fb}^{-1}$ of $p\bar{p}$ collisions. The general features of the event selection requirements are as follows. We require exactly one well-reconstructed charged-lepton candidate (electron or muon) with $p_T > 20\,\text{GeV}/c$, an imbalance in the total event transverse momentum (missing transverse energy [25]) $\not\!\!E_T > 20\,\text{GeV}$, and four or more calorimeter-energy clusters (jets [26]), three with $E_T > 20\,\text{GeV}$ and the fourth with $E_T > 12\,\text{GeV}$, in the central part of the detector ($|\eta| < 2.0$). We further require that at least one of the jets be identified (tagged) as having a displaced vertex resulting from the decay of a bottom-quark meson, which is produced from the dominant top-quark decay $t \to Wb$. Further details on the online and offline event selection requirements are in [1]. The resulting data set is enriched in $t\bar{t}$ events, but it contains non-$t\bar{t}$ background events as well, dominated by events in which a W boson is produced in association with hadron jets. The rates and differential distributions of all the sources of non-$t\bar{t}$ backgrounds are well understood [1]. We expect to observe 2750 ± 427 $t\bar{t}$ events and 1026 ± 210 non-$t\bar{t}$ background events, and we observe 3864 $t\bar{t}$ candidate events.

We reconstruct the top quark and the top anti-quark from their decay products, using the measured momentum of the lepton and the four jets, as well as the missing transverse energy. We fit each possible jet-to-parton assignment to the $t\bar{t}$ hypothesis. We require that two of the jets be consistent with the decay of a W boson of mass $80.4\,\text{GeV}/c^2$ and that the lepton and missing transverse

energy also be consistent with the decay of a W boson. We further require that each reconstructed W boson, when paired with one of the remaining jets, be consistent with the decay of a top quark of mass $172.5\,\mathrm{GeV}/c^2$ [27]. The jet-to-parton assignment which is most consistent with this $t\bar{t}$ hypothesis is used to calculate the top-quark production angle as measured in the detector, $\cos\theta_t^{\mathrm{det}}$, for each event.

We exploit the orthonormality of the Legendre polynomials to estimate the Legendre moments without performing a fit. Given a distribution $f(\cos\theta_t)$, the Legendre moments of f are

$$a_\ell = \frac{2\ell+1}{2}\int_{-1}^{1} d(\cos\theta_t) f(\cos\theta_t) P_\ell(\cos\theta_t). \qquad (3)$$

The data are described by an empirical distribution [28], $f(\cos\theta_t^{\mathrm{det}}) = \sum_i \delta(\cos\theta_t^{\mathrm{det}} - \cos\theta_{t,i}^{\mathrm{det}})$, where $\delta(x)$ is the Dirac δ function and the index i runs over the events in the data set. Using this distribution in Eq. (3) greatly simplifies the integration due to the Dirac delta functions, so the moments of the observed $\cos\theta_t^{\mathrm{det}}$ distribution are

$$a_\ell^{\mathrm{det}} = \frac{2\ell+1}{2}\sum_i P_\ell(\cos\theta_{t,i}^{\mathrm{det}}). \qquad (4)$$

Then, the estimate of the moments is

$$a_\ell = \sum_m K_{\ell m}\left(\sum_i P_m(\cos\theta_{t,i}^{\mathrm{det}}) - a_m^{\mathrm{BG}}\right), \qquad (5)$$

where a_m^{BG} represents the Legendre moments of the distribution of $\cos\theta_t^{\mathrm{det}}$ predicted by the background model, and $K_{\ell m}$ is a correction matrix that accounts for the finite resolution of the detector and for the non-uniform detector acceptance and selection efficiency. The matrix K is developed from a sample of fully-simulated $t\bar{t}$ Monte Carlo events generated by the POWHEG NLO SM generator [29]. It describes the response of the detector and the effects of the event selection requirements. No smoothing or regularization is applied in this correction procedure, in contrast to the correction procedure of [1].

The statistical uncertainties on the moments are given by a root-mean-square covariance matrix including correlations. In order to estimate the effect from each of several sources of systematic uncertainty in the model assumptions, we vary the corresponding nuisance parameter that alters either the background prediction or correction matrix, and then perform the full correction procedure again. The resulting parton-level moments estimate is compared to the unvaried moments, and then the covariance matrix describing the uncertainty on the measurement is $\sigma_{m\ell} = \delta_m\delta_\ell$, where $\delta_\ell \equiv a_\ell^{\mathrm{varied}} - a_\ell^{\mathrm{nominal}}$. We study systematic shifts due to the uncertainty in the jet-energy scale, the rate of the backgrounds, the shape of the backgrounds, the modeling of parton showering, the modeling of color reconnection, the modeling of initial- and final-state radiation, and the parton distribution functions of the proton and antiproton. We sum the resulting covariance matrices and add them to the statistical covariance matrix to obtain a covariance matrix that fully describes the uncertainty of the measurement of the parton-level Legendre moments. The eigenvalues and eigenvectors of the covariance matrix [30] can be used to calculate a χ^2 goodness-of-fit statistic with eight degrees of freedom in order to perform fits to the data.

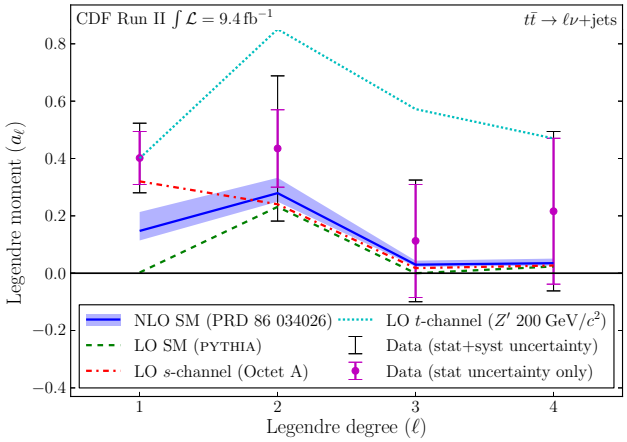

FIG. 2. Measured Legendre moments a_1–a_4, with theory predictions overlaid.

TABLE I. Measured Legendre moments a_1–a_8, with NLO SM prediction. The uncertainty on the measured moments is the total uncertainty from statistical and systematic sources. The uncertainty on the prediction reflects reasonable variations in the renormalization scale [5].

ℓ	a_ℓ (obs)	a_ℓ (pred)
1	0.40±0.12	$0.15^{+0.07}_{-0.03}$
2	0.44±0.25	$0.28^{+0.05}_{-0.03}$
3	0.11±0.21	$0.030^{+0.014}_{-0.007}$
4	0.22±0.28	$0.035^{+0.016}_{-0.008}$
5	0.11±0.33	$0.005^{+0.002}_{-0.001}$
6	0.24±0.40	$0.006^{+0.002}_{-0.003}$
7	−0.15±0.48	$-0.003^{+0.001}_{-0.001}$
8	0.16±0.65	$-0.0019^{+0.0003}_{-0.0003}$

The parton-level Legendre moments are shown in Fig. 2 and in Table I. We observe good agreement within the uncertainties with the NLO SM prediction for moments a_2–a_8, but a_1 is in excess of the prediction. That is, a mild excess is observed in the differential cross section in the term linear in $\cos\theta_t$, while all other terms are as predicted by the SM. The LO SM prediction is strongly disfavored by the linear term, with a significance of more than three standard deviations. The benchmark t-channel model, "Z' 200", is disfavored by a_2 and a_3. The benchmark s-

channel model, "Octet A", is in good agreement with the data.

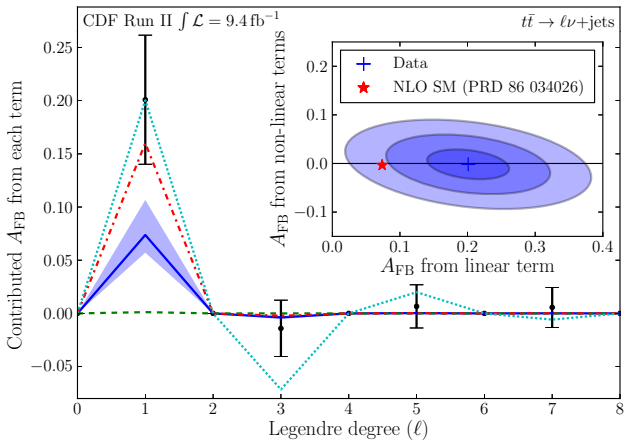

FIG. 3. Absolute contributions of the Legendre moments to the A_{FB}, with theory predictions overlaid. The lines and symbols are the same as in Fig. 2. The inset shows the 1-, 2-, and 3-standard-deviation uncertainty ellipses.

We determine the contribution of each Legendre moment to the A_{FB} from the inherent asymmetry of each polynomial (Fig. 3). The observed A_{FB} $(19.9 \pm 5.7)\,\%$ is completely dominated by the excess linear term, $a_1 \cos\theta_t$, which contributes $(20.1 \pm 6.1)\,\%$. The A_{FB} contributed by the non-linear asymmetric terms a_3, a_5, and a_7 is negligible $(-0.2 \pm 3.1)\,\%$, and is consistent with the SM prediction (7.3 % from the linear term, $-0.3\,\%$ from the non-linear terms). The correlation between the measurements of A_{FB} from the linear and non-linear terms is $-29\,\%$.

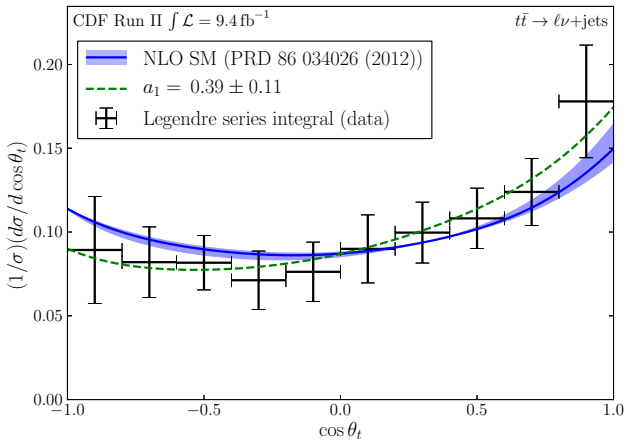

FIG. 4. Fraction of cross section accruing in 10 bins of $\cos\theta_t$, obtained by integrating the series of Legendre polynomials over the width of each bin.

A more traditional picture of the differential cross section (Fig. 4) is obtained by integrating the Legendre series over intervals (bins) in $\cos\theta_t$. This shows the fraction of the total cross section that accrues in each bin. The uncertainties are strongly correlated, and they are dominated by the large uncertainties on the high-degree Legendre moments.

Because the non-linear moments, a_2–a_8, are in good agreement within the uncertainties with the NLO SM prediction, we may obtain a more precise, but model-dependent, estimate of the linear term by explicitly assuming that the non-linear moments are as predicted by the NLO SM calculation. Using the covariance matrix and the fitting procedure described in [30], we fit to the measured moments, taking the NLO SM prediction for the non-linear moments with their scale uncertainties as a prior assumption, obtaining $a_1 = 0.39 \pm 0.11$ (including statistical and systematic uncertainty). Through the correlations among the measured moments, this reduces the uncertainty on a_1 by about 10 % while shifting the central value less than 3 %. The resulting curve is also shown in Fig. 4.

In conclusion, we have presented the first measurement of the top-quark-pair production differential cross section, $d\sigma/d(\cos\theta_t)$, in $p\bar{p}$ collisions at $\sqrt{s} = 1.96\,\mathrm{TeV}$ as a function of the production angle of the top quark. In order to probe the origin of the top-quark-production asymmetry, we decompose the angular form into Legendre polynomials. We observe that the coefficient of the $\cos\theta_t$ term in the differential cross section, $a_1 = 0.40 \pm 0.12$, is in excess of the NLO SM prediction, $0.15^{+0.07}_{-0.03}$, while the remainder of the differential cross section is in good agreement within the uncertainties with the NLO SM prediction. The top-quark forward-backward asymmetry is thus completely dominated by the linear term. The result constrains t-channel explanations of the asymmetry and favors asymmetry models with strong s-channel components.

We thank T. Tait, S. Jung, W. Bernreuther, and Z.-G. Si for their assistance in preparing the theoretical models and calculations used in this Letter, and T. Rizzo for helpful conversations. We also thank the development teams of SCIPY, PYTABLES, MATPLOTLIB, and IPYTHON for their useful tools [31].

We thank the Fermilab staff and the technical staffs of the participating institutions for their vital contributions. This work was supported by the U.S. Department of Energy and National Science Foundation; the Italian Istituto Nazionale di Fisica Nucleare; the Ministry of Education, Culture, Sports, Science and Technology of Japan; the Natural Sciences and Engineering Research Council of Canada; the National Science Council of the Republic of China; the Swiss National Science Foundation; the A.P. Sloan Foundation; the Bundesministerium für Bildung und Forschung, Germany; the Korean World Class University Program, the National Research Foundation of Korea; the Science and Technology Facilities Council and the Royal Society, UK; the Russian Foundation for

Basic Research; the Ministerio de Ciencia e Innovación, and Programa Consolider-Ingenio 2010, Spain; the Slovak R&D Agency; the Academy of Finland; the Australian Research Council (ARC); and the EU community Marie Curie Fellowship contract 302103.

[1] T. Aaltonen *et al.* (CDF Collaboration), Phys. Rev. D **87**, 092002 (2013).

[2] V. M. Abazov *et al.* (D0 Collaboration), Phys. Rev. D **84**, 112005 (2011).

[3] *CP* is the simultaneous transformation of charge conjugation and parity.

[4] S. L. Glashow, Nucl. Phys. **22**, 579 (1961); S. Weinberg, Phys. Rev. Lett. **19**, 1264 (1967); A. Salam, in *Elementary Particle Theory*, edited by N. Svartholm (Almquist and Wiksell, Stockholm, 1968) p. 367.

[5] W. Bernreuther and Z.-G. Si, Phys. Rev. D **86**, 034026 (2012); W. Bernreuther (private communication).

[6] J. H. Kuhn and G. Rodrigo, Phys. Rev. Lett. **81**, 49 (1998).

[7] S. J. Brodsky and X.-G. Wu, Phys. Rev. D **85**, 114040 (2012).

[8] W. Hollik and D. Pagani, Phys. Rev. D **84**, 093003 (2011).

[9] J. H. Kuhn and G. Rodrigo, J. High Energy Phys. 01 (2012) 063.

[10] A. V. Manohar and M. Trott, Phys. Lett. B **711**, 313 (2012).

[11] J. F. Kamenik, J. Shu, and J. Zupan, Eur. Phys. J. C **72**, 2102 (2012).

[12] E. L. Berger, Argonne National Laboratory Report ANL-HEP-CP-12-87, 2013 (unpublished).

[13] S. Chatrchyan *et al.* (CMS Collaboration), Phys. Lett. B **717**, 129 (2012).

[14] G. Aad *et al.* (ATLAS Collaboration), Euro. Phys. J. C **72**, 2039 (2012).

[15] We normalize the Legendre polynomials so that $\frac{2\ell+1}{2}\int_{-1}^{1} dx P_\ell(x)P_{\ell'}(x) = \delta_{\ell\ell'}$, where $\delta_{\ell\ell'}$ is the Kronecker delta.

[16] M. Jacob and G.C. Wick, Ann. Phys. (N.Y.) **7**, 404 (1959); **281**, 774 (2000).

[17] T. Sjöstrand, S. Mrenna, and P. Skands, J. High Energy Phys. 05 (2006) 026, we use PYTHIA version 6.216.

[18] T. Aaltonen *et al.* (CDF Collaboration), Phys. Rev. D **83**, 112003 (2011).

[19] S. Jung, A. Pierce, and J. D. Wells, Phys. Rev. D **83**, 114039 (2011).

[20] M. I. Gresham, I.-W. Kim, and K. M. Zurek, Phys. Rev. D **83**, 114027 (2011).

[21] S. Mandelstam, Phys. Rev. **112**, 1344 (1958).

[22] J. Alwall, P. Demin, S. de Visscher, R. Frederix, M. Herquet, F. Maltoni, T. Plehn, D. L. Rainwater, and T. Stelzer, J. High Energy Phys. 09 (2007) 028.

[23] D. E. Acosta *et al.* (CDF Collaboration), Phys. Rev. D **71**, 032001 (2005).

[24] We use a cylindrical coordinate system with the origin at the center of the CDF detector, z pointing in the direction of the proton beam, θ and ϕ representing the polar and azimuthal angles, respectively, and pseudorapidity defined by $\eta = -\ln\tan(\theta/2)$. The transverse momentum p_T (transverse energy E_T) is defined to be $p\sin\theta$ ($E\sin\theta$).

[25] The calorimeter missing E_T ($\vec{\not\!\!E}_T$(cal)) is defined by the sum over calorimeter cells, $\vec{\not\!\!E}_T(\mathrm{cal}) = -\sum_i E_T^i \hat{n}_i$, where i is calorimeter cell number with $|\eta| < 3.6$, $\hat{n}_i$ is a unit vector perpendicular to the beam axis and pointing at the ith calorimeter cell. The reconstructed missing energy, $\vec{\not\!\!E}_T$, is derived by subtracting from $\vec{\not\!\!E}_T$(cal) the energies associated with components of the event not registered by the calorimeter, such as muons and jet energy adjustments. $\not\!\!E_T$(cal) and $\not\!\!E_T$ are the scalar magnitudes of $\vec{\not\!\!E}_T$(cal) and $\vec{\not\!\!E}_T$, respectively.

[26] A. Bhatti *et al.*, Nucl. Instrum. Methods A **566**, 375 (2006).

[27] A. Abulencia *et al.* (CDF Collaboration), Phys. Rev. D **73**, 032003 (2006).

[28] A. Kolmogorov, G. Ist. Ital. Attuari **4**, 83 (1933); V. I. Smirnov, Byull. Moskov. Gos. Univ. Ser. A **2**, 2 (1938).

[29] S. Frixione, P. Nason, and G. Ridolfi, J. High Energy Phys. 09 (2007) 126.

[30] See Supplemental Material at [URL will be inserted by publisher] for the eigenvalues and eigenvectors of the covariance matrix describing the correlations and uncertainty of this measurement.

[31] E. Jones *et al.*, "SciPy: Open source scientific tools for Python," (2001), `http://www.scipy.org/`; F. Alted *et al.*, "PyTables: Hierarchical datasets in Python," (2002), `http://www.pytables.org/`; J. D. Hunter, Comput. Sci. Eng. **9**, 90 (2007), `http://matplotlib.org`; F. Pérez and B. E. Granger, Comput. Sci. Eng. **9**, 21 (2007), `http://ipython.org`.